J|A|C|S COMMUNICATIONS

Published on Web 09/10/2010

Tunability in Polyatomic Molecule Diffusion through Tunneling versus Pacing

Zhihai Cheng, Eric S. Chu, Dezheng Sun, Daeho Kim, Yeming Zhu, MiaoMiao Luo, Greg Pawin, Kin L. Wong, Ki-Young Kwon, Robert Carp, Michael Marsella, and Ludwig Bartels*

Department of Chemistry, University of California, Riverside, California 92521

Received April 2, 2010; E-mail: ludwig.bartels@ucr.edu

Abstract: The diffusion temperature of molecular 'walkers', molecules that are capable of moving unidirectionally across a substrate violating its symmetry, can be tuned over a wide range utilizing extension of their aromatic backbone, insertion of a second set of substrate linkers (converting bipedal into quadrupedal species), and substitution on the ring. Density functional theory simulation of the molecular dynamics identifies the motion of the quadrupedal species as pacing (as opposed to trotting or gliding). Knowledge about the diffusion mode allows us to draw conclusions on the relevance of tunneling to the surface diffusion of polyatomic organic molecules.

The development of molecular machines as realization of the ultimate miniaturization of macroscopic devices has become a research topic of general and widespread interest. Molecular machines are common in the biochemical arena (F1-motor of ATP synthase, proton pump in cell membranes, transcription polymerase, kinesin motor proteins, etc.). Much smaller and easier to handle molecules have been synthesized to resemble macroscopic devices such as gears,[1] cars,[2] ratchets,[3] walkers,[4−6] turnstiles,[7,8] pinwheels,[9] shuttles,[10] 'sky-hooks',[11] and wheel-barrows[12] when adsorbed at a metal surface.[13−16] For surface molecular machinery to obtain ultimate utility, it is necessary that their motion is reliable and their rate of motion is tunable in a predetermined fashion to the task at hand. Here we report on a class of molecules that allows us the study of the transition from thermally assisted tunneling diffusion to purely thermal diffusion[17] and permits tuning of the diffusion temperature between 20 and 80 K.

In previous work anthraquinone[6] (AQ) (and its sulfur counterpart dithioanthracene,[5] DTA) has been shown to diffuse on 6-fold symmetric Cu(111) exclusively along the high-symmetry direction indicated by its aromatic moiety, i.e. violating the substrate symmetry, which is accomplished by sequential placement of its chalcogen substrate linkers, a process dubbed 'walking'. While AQ movement proved useful in carrying cargo, its very low apparent diffusion prefactor of just $10^{2.4}$ Hz and barrier of 0.02 eV indicate a diffusion mode that is not well understood. Here we show that modification of AQ can lead either to similar or to much higher diffusion barriers and prefactors, depending on whether the resultant molecule can adopt a diffusion mode, in which tunneling of a single atom only can forward it.

We investigated the surface diffusion of pentaquinone (PQ), pentacenetetrone (PT), and a derivative of PT carrying methyl groups at diagonally opposed ends of the aromatic backbone, dimethylpentacenetetrone (DPT). The first two species were obtained commercially, and DPT was synthesized through dimerization of suitably substituted naphtaquions. While PQ differs from AQ only by extension of the ring system and thus may be expected to diffuse in a similar way across a surface, PT and DPT have four substrate linkers and potential docking sites for molecular cargo, inviting the question: in which fashion does a quadrupedal species move across a surface? Will it be in a walking style at all? And if it is a walking style, which gait will its legs adopt: trotting, in which diagonally opposed legs move in unison, or pacing, in which both legs on one side of the molecule move together?

All measurements in this manuscript were performed in a scanning tunneling microscopy (STM) instrument capable of imaging molecular diffusion at 8 K and above in ultrahigh vacuum. Preparation of the Cu(111) sample involved sequences of sputtering and annealing, followed by cooling to 80 K. Deposition of the molecules from a glass capillary proceeded on the cryogenic sample followed by annealing to close to room temperatures to desorb inevitable solvent residues. All coverages were ~1 molecule per 100 substrate atoms, so that isolated molecules can be investigated. Temperatures were measured by a silicon diode attached to the STM scanner, which in turn had been calibrated by replacing the STM tip with a silicon diode in the tip-holder−sample junction. In combination, this results in a temperature uncertainty of ±1 K.

All density functional theory simulations (DFT) utilized the VASP code[18] with the generalized-gradient approximation[19] for the exchange-correlation functional and the plane-wave pseudopotential method[20] with ultrasoft pseudopotentials.[21] Our calculations use a 4×8 substrate atoms supercell with 4 substrate layers that provides a sufficiently large lateral extent to prevent intermolecular interactions despite circular boundary conditions. The atom positions were optimized so that all forces in the system are smaller than 0.04 eV/Å.

We find that PQ adsorbs on Cu(111) very similar to AQ,[6] i.e. with its anthracene body aligned with one of the substrate atomic rows (Figure 1a). In STM images it appears as an elongated protrusion with a slightly narrower waist at the carbonyl group positions. DFT simulation of its adsorption configuration shows its carbonyl substrate linkers pinned to the substrate with the remainder of the molecule bent upward (Figure 1c), similar to AQ. Figure 1b and d show an STM image of several PT molecules on a Cu(111) surface and a cross section of the PT adsorption configuration obtained by integrating the charge density across planes normal to the surface and the molecule. The molecular axis is aligned with one of the atomic rows of the substrate. Its four carbonyl oxygen legs come to rest on the surface, pulling the second and fourth aromatic ring down onto the substrate, while allowing the terminal rings to lift upward. DPT adsorbs similar to PT on Cu(111).

Sequences of STM measurements reveal that PQ, PT, and DPT diffuse exclusively along the axis indicated by their aromatic moiety, similar to AQ.[6] The Supporting Information shows a movie. We acquired several days of diffusion data on each of the molecules; in several thousand diffusion events investigated, no perpendicular motion or rotation has been observed.

10.1021/ja1027343

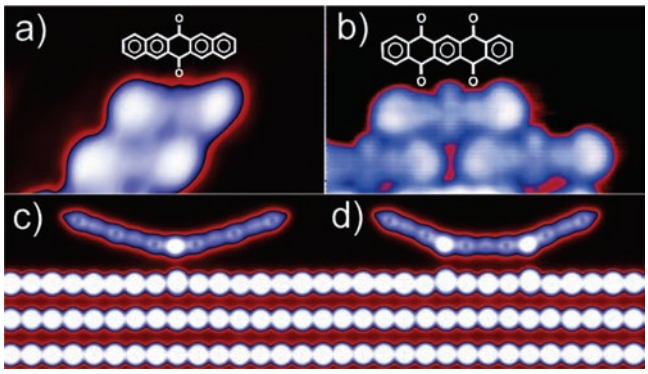

Figure 1. (a,b) STM images of PQ (a) and PT (b) on Cu(111); (c,d) Integrated charge density from DFT simulation[5,22] of PQ (c) and PT (d) on Cu(111). The carbonyl groups pin PQ and PT to the substrate leaving their peripheral portions free to angle upward. STM image parameters: (a) 93 pA, −1.7 V, 37 Å × 22 Å; (b) 130 pA, −1.1 V, 32 Å × 19 Å. Note that in panels c,d the substrate atoms appear twice as close because of the offset of alternating atom rows on the fcc(111) surface.

Plotting the molecular diffusion rate versus the experimental temperature leads to the Arrhenius plot of Figure 2, which, in addition to the PQ, PT, and DPT, also shows the diffusion rate of AQ for ref 6. The statistical error is smaller than the data markers. From these data, diffusion barriers of 0.02 eV ± 0.01 and 0.03 eV ± 0.01 eV for AQ and PQ, respectively, and of 0.13 eV ± 0.02 and 0.19 eV ± 0.02 eV for PT and DPT, respectively, can be extracted. Although the largest variation in diffusion barrier is found between bipedal and quadrupedal species, the difference in diffusion barrier induced by methyl substitution and elongation of the ring system is substantial (i.e., ∼50% each). For example, extrapolation of the diffusion rate of the methylated species to the unmethylated one indicates almost a 1×10^6-fold difference in diffusion rate. The effect of methylation is even sufficient to put the observation of uniaxial diffusion within reach of LN_2 cooling. These results make it clear that terminal methyl substitution and backbone elongation, despite their chemically inert nature, and remote location from the fulcrum of the motion, are very sensitive handles for tuning the diffusion rates of walking molecules.

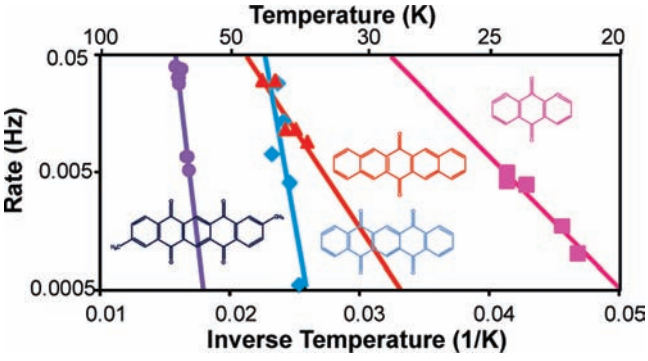

Figure 2. Arrhenius plot of the uniaxial motion of AQ (pink), PQ (red), PT (blue), and DPT (purple).

The difference between bipedal and quadrupedal species is even more striking, if the prefactors are compared. For AQ and PQ they are $10^{2.4\pm1}$ and $10^{2.3\pm1}$, respectively, whereas for PT and DPT they are both $10^{13\pm1}$ Hz. The prefactors for the bipedal species are much lower than the conventional $10^{10}-10^{13}$ Hz, yet low prefactors have been reported in a number of STM diffusion experiments at low temperatures: CO/Cu(111), $\sim10^7$ Hz;[23] CO chevrons/Cu(111), $\sim10^5$ Hz;[24] CO/Cu(110), $\sim10^7$ Hz;[25] Al/Au(111), $\sim10^3$ Hz[26]). A concerted lowering of prefactors and barrier has been described already 70 years ago, named the Meyer Neldel rule or compensation effect,[27,28] and has since been observed for a range of phenomena including conductivity of semiconductor, mobility of polymers, grain and phase-boundary motion, etc.[29] Yet the magnitude of reduction observed here is larger than typical Meyer Neldel effects, raising the question what in particular sets quadrupedal motion apart from that of bipedal species.

To this end, we performed DFT simulations of how PT overcomes the diffusion barrier. Starting out from the initial, minimized configuration, we move the substrate linkers successively by 0.1−0.2 Å at a time followed by renewed minimization of the entire system so that all forces are smaller than 0.04 eV/Å, while keeping only the forward motion of the manipulated oxygen atoms fixed. In a previous mapping of the diffusion potential for AQ and DTA we showed that the molecules move by alternatingly stepping their substrate linkers, angling the molecule with regards to the substrate atomic rows.[5,6] For the quadrupedal species, mapping of the entire parameter space is computationally prohibitive, because it is not two-dimensional as in the case of AQ but four-dimensional. Rather we investigate the diffusion barrier along three potential pathways: the first, in which two diagonally opposed substrate linkers move at a time resembling the gait of trotting (Figure 3 b); the second, in which two adjacent substrate linkers move at a time resembling pacing (Figure 3c); the last, in which the molecule glides across the surface moving all oxygen atoms forward simultaneously (Figure 3d). Using the mean forward motion of the substrate linkers as a reaction coordinate, the diffusion barriers of Figure 3e result. The Supporting Information contains movies illustrating these motion modes.

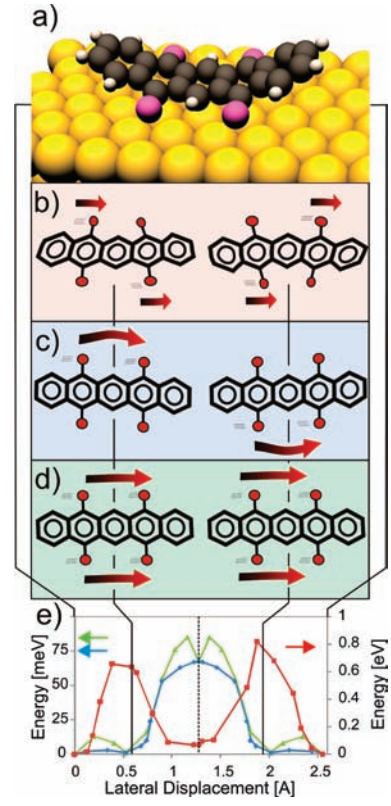

Figure 3. Setup of PT on Cu(111) as obtained from DFT-based minimization (a) and schematic representation of trotting (red), pacing (blue), and gliding (green). Panel e shows the corresponding energy barriers, with trotting on the right *y*-axis and pacing as well as gliding on the left axis.

Each of the diffusion pathways is associated with more than one barrier. During trotting, only one pair of diagonally opposed substrate linkers moves whereas the other stays stationary, leading to a distortion of the molecule. The maximum distortion is reached at 1/4 (and 3/4) of the step distance coinciding with the maximum barrier height of 0.7−0.8 eV. At the diffusion midpoint, the distortion of the molecule is released and the total energy is at a local minimum, despite the fact that here the interaction with the substrate is not optimal. The diffusion barrier encountered during trotting is significantly higher than the measured value, and it is prohibitive at the temperatures of our experiments. It reflects the great energetic cost associated with distorting the molecule's aromatic backbone.

On the gliding pathway (and to a lesser degree on the pacing pathway), initial displacement from the equilibrium adsite encounters a small barrier. While pacing, the second set of substrate linkers starts to move once the first set reaches 1/4 of the diffusion distance. At the diffusion quarterpoint ($\approx$ 0.6 Å) the molecular setups for pacing and gliding merge at an energetic minimum. Similarly, all diffusion pathways merge at the diffusion halfpoint and the molecule is aligned parallel to the diffusion direction. In gliding, PT approaches this point via a considerable barrier, whereas, in pacing, the molecule angles itself barrierless into this configuration. In contrast to trotting motion, pacing and gliding motions are inversion symmetric at the diffusion midpoint.

The absolute height of the simulated diffusion barrier of $\sim$0.07 eV is somewhat lower than the experimental value of 0.13 eV; van der Waals (vdW) interactions are absent from our DFT simulations for reason of computational feasibility, although they are known to contribute substantially to the acene−substrate interaction, thus explaining the difference in total barrier.[30,31] While we wish to caution that this may also impact our assignment of the gait, we believe that the 0.02 eV difference in energy between pacing and gliding will not be superseded by vdW interactions given their typically slow spatial variation.[30]

Our simulations indicate that the motion of the molecular backbone during diffusion is quite similar for bipedal and quadrupedal species, yet in the quadrupedal motion the substrate linkers need to occupy inequivalent adsites. In the pacing gait, two substrate linkers always need to move at the same time, in contrast to the energetically prohibitive trotting, where sequential movement of the substrate linkers is conceivable. What implications does this have for understanding the variation in diffusion prefactors between bipedal and quadrupedal species?

Tunneling has been discussed as a mechanism for low-temperature diffusion of hydrogen atoms and also for CO diffusion on Cu(111) by Eigler's group,[24,32,33] who found indications that the mass m relevant for tunneling is exclusively that of the substrate-attached atom (i.e., carbon in the case of CO molecules) and not the entire molecule. Thus, in the case of the molecules investigated here, the tunneling species may just be the oxygen (carbonyl) substrate linkers. Tunneling can require thermal activation, i.e. once the molecule has thermally reached a certain vibrationally excited state, the remaining barrier height E_{atom} and depth d are crossed via tunneling.[24] An Arrhenius analysis will still result in a straight line, but the barrier height E_{barr} obtained corresponds to the energy of the required vibrational activation. The apparent attempt frequency is the product of the attempt frequency leading to occupation of the vibrationally excited state and the tunneling probability P from that state across the barrier.[34] P can be estimated in the Wentzel−Kramers−Brillouin (WKB) approximation:[24]

$$P = \exp\left(-{}^{2}/_{\hbar} \int_0^d \sqrt{2mE_{\mathrm{atom}}(x)}\, \mathrm{d}x\right)$$

Assuming the central portion of the pacing barrier (Figure 3e) as $E_{\mathrm{atom}}(x) + E_{\mathrm{barr}}$, a tunneling probability of $\sim 10^{-10}$ results. Thus, if the rate at which the bipedal AQ species approaches the vibrationally excited state is assumed to be a typical value of $10^{12}-10^{13}$ Hz, an apparent attempt frequency of $10^{2}-10^{3}$ Hz is expected, which corresponds to the values measured here.

Why then do we observe low prefactors for the bipedal species and conventional ones for the quadrupedal species? The simulation shows that the molecular distortion required to place the substrate linkers sequentially (as it is possible in the trotting gait) is energetically prohibitive. Pacing, however, requires concerted motion of both substrate linkers on one side of the molecule; yet concerted tunneling of them has a probability of $P^2 \approx 10^{-20}$, too unlikely to occur. Thus, tunneling is only an option for a molecule, in whose motion no concerted displacement of substrate linkers is required.

The combination of modeling of the diffusion mode and calculation of the tunneling probability provides a strong argument in favor of the relevance of tunneling for the bipedal species. Moreover, the apparent barriers obtained from the Arrhenius fit of AQ and PQ diffusion of 0.02 and 0.03 eV are a much better match for vibrational modes of oxygen atoms at surfaces, as required for thermally assisted tunneling, than for actual diffusion barriers.[35]

Acknowledgment. Supported by U.S. Department of Energy Grant DE-FG02-07ER15842 and by NSF Grant 0749949. Computational resources were made available by the NSF Teragrid and the Beran group at UCR.

Supporting Information Available: Description of synthetic methods; movies and animation of the molecular motion. This material is available free of charge via the Internet at http://pubs.acs.org.

References

(1) Gimzewski, J. K.; Joachim, C.; Schlittler, R. R.; Langlais, V.; Tang, H.; Johannsen, I. *Science* **1998**, *281*, 531–533.
(2) Shirai, Y.; Osgood, A. J.; Zhao, Y. M.; Kelly, K. F.; Tour, J. M. *Nano Lett.* **2005**, *5*, 2330–2334.
(3) Kelly, T. R.; De Silva, H.; Silva, R. A. *Nature* **1999**, *401*, 150–152.
(4) von Delius, M.; Geertsema, E. M.; Leigh, D. A. *Nat. Chem.* **2009**, *2*, 96–101.
(5) Kwon, K. Y.; Wong, K. L.; Pawin, G.; Bartels, L.; Stolbov, S.; Rahman, T. S. *Phys. Rev. Lett.* **2005**, *95*, 166101.
(6) Wong, K. L.; Pawin, G.; Kwon, K. Y.; Lin, X.; Jiao, T.; Fawcett, R.; Solanki, U.; Bartels, L.; Stolbov, S.; Rahman, T. S. *Science* **2007**, *315*, 1391–1393.
(7) Moore, J. S. *Acc. Chem. Res.* **1997**, *30*, 402–413.
(8) Baber, A. E.; Tierney, H. L.; Sykes, E. C. H. *ACS Nano* **2008**, *2*, 2385–2391.
(9) Vaughan, O. P. H.; Williams, F. J.; Bampos, N.; Lambert, R. M. *Angew. Chem., Int. Ed.* **2006**, *45*, 3779–3781.
(10) Balzani, V.; Credi, A.; Raymo, F. M.; Stoddart, J. F. *Angew. Chem., Int. Ed.* **2000**, *39*, 3348–3391.
(11) Horch, S.; Lorensen, H.; Helveg, S.; Laegsgaard, E.; Stensgaard, I.; Jacobsen, K.; Norskov, J.; Besenbacher, F. *Nature* **1999**, *398*, 134–136.
(12) Grill, L.; Rieder, K. H.; Moresco, F.; Rapenne, G.; Stojkovic, S.; Bouju, X.; Joachim, C. *Nat. Nanotechnol.* **2007**, *2*, 95–98.
(13) Kottas, G. S.; Clarke, L. I.; Horinek, D.; Michl, J. *Chem. Rev.* **2005**, *105*, 1281–1376.
(14) van Delden, R. A.; ter Wiel, M. K. J.; Pollard, M. M.; Vicario, J.; Koumura, N.; Feringa, B. L. *Nature* **2005**, *437*, 1337–1340.
(15) Kay, E. R.; Leigh, D. A.; Zerbetto, F. *Angew. Chem., Int. Ed.* **2007**, *46*, 72–191.
(16) Liu, Y.; Flood, A. H.; Bonvallett, P. A.; Vignon, S. A.; Northrop, B. H.; Tseng, H. R.; Jeppesen, J. O.; Huang, T. J.; Brough, B.; Baller, M.; Magonov, S.; Solares, S. D.; Goddard, W. A.; Ho, C. M.; Stoddart, J. F. *J. Am. Chem. Soc.* **2005**, *127*, 9745–9759.
(17) Repp, J.; Meyer, G.; Rieder, K.; Hyldgaard, P. *Phys. Rev. Lett.* **2003**, *91*, 206102.
(18) Kresse, G.; Hafner, J. *Phys. Rev. B* **1993**, *47*, 558–561.
(19) Perdew, J. P.; Wang, Y. *Phys. Rev. B* **1992**, *45*, 13244–13249.
(20) Payne, M. C.; Teter, M. P.; Allan, D. C.; Arias, T. A.; Joannopoulos, J. D. *Rev. Mod. Phys.* **1992**, *64*, 1045–1097.
(21) Vanderbilt, D. *Phys. Rev. B* **1990**, *41*, 7892–7895.

(22) Pawin, G.; Wong, K. L.; Kim, D.; Sun, D. Z.; Bartels, L.; Hong, S.; Rahman, T. S.; Carp, R.; Marsella, M. *Angew. Chem., Int. Ed.* **2008**, *47*, 8442–8445.
(23) Wong, K. L.; Rao, B. V.; Pawin, G.; Ulin-Avila, E.; Bartels, L. *J. Chem. Phys.* **2005**, *123*, 201102.
(24) Heinrich, A.; Lutz, C.; Gupta, J.; Eigler, D. *Science* **2002**, *298*, 1381–1387.
(25) Briner, B.; Doering, M.; Rust, H.; Bradshaw, A. *Science* **1997**, *278*, 257–260.
(26) Fischer, B.; Brune, H.; Barth, J. V.; Fricke, A.; Kern, K. *Phys. Rev. Lett.* **1999**, *82*, 1732–1735.
(27) Meyer, W.; Neldel, H. *Phys. Z.* **1937**, *38*, 1014–1019.
(28) Boisvert, G.; Lewis, L. J.; Yelon, A. *Phys. Rev. Lett.* **1995**, *75*, 469–472.
(29) *Defect and Diffusion Forum: The Meyer-Neldel Rule*; Fisher, D. J., Ed.; Trans Tech Publications Inc.: Zurich, Switzerland, 2001; Vols. 192−193.
(30) Berland, K.; Einstein, T. L.; Hyldgaard, P. *Phys. Rev. B* **2009**, *80*, 155431.
(31) Mercurio, G.; McNellis, E. R.; Martin, I.; Hagen, S.; Leyssner, F.; Soubatch, S.; Meyer, J.; Wolf, M.; Tegeder, P.; Tautz, F. S.; Reuter, K. *Phys. Rev. Lett.* **2010**, *104*, 036102.
(32) Kua, J.; Lauhon, L.; Ho, W.; Goddard, W. *J. Chem. Phys.* **2001**, *115*, 5620–5624.
(33) Lauhon, L.; Ho, W. *Phys. Rev. Lett.* **2000**, *85*, 4566–4569.
(34) Price, P. J. *Am. J. Phys.* **1998**, *66*, 1119–1122.
(35) Witte, G.; Braun, J.; Nowack, D.; Bartels, L.; Neu, B.; Meyer, G. *Phys. Rev. B* **1998**, *58*, 13224–13232.

JA1027343